Coastal Engineering 56 (2009) 1084–1096

Contents lists available at ScienceDirect

Coastal Engineering

journal homepage: www.elsevier.com/locate/coastaleng

A numerical model of nearshore waves, currents, and sediment transport

Pham Thanh Nam [a,b,*], Magnus Larson [a], Hans Hanson [a], Le Xuan Hoan [a,b]

[a] Department of Water Resources Engineering, Lund University, Box 118, S-22100, Lund, Sweden
[b] Center for Marine Environment, Research and Consultation, Institute of Mechanics, Vietnamese Academy of Science and Technology, 264 Doi Can, Hanoi, Vietnam

ARTICLE INFO

Article history:
Received 29 August 2008
Received in revised form 9 April 2009
Accepted 15 June 2009
Available online 27 August 2009

Keywords:
Mathematical modeling
Random wave
Nearshore current
Swash zone
Sediment transport
Surface roller

ABSTRACT

A two-dimensional numerical model of nearshore waves, currents, and sediment transport was developed. The multi-directional random wave transformation model formulated by Mase [Mase, H., 2001. Multi-directional random wave transformation model based on energy balance equation. Coastal Engineering Journal 43(4), 317-337.] based on an energy balance equation was employed with an improved description of the energy dissipation due to breaking. In order to describe surface roller effects on the momentum transport, an energy balance equation for the roller was included following Dally and Brown [Dally, W.R., Brown, C.A., 1995. A modeling investigation of the breaking wave roller with application to cross-shore currents. Journal of Geophysical Research 100(C12), 24873-24883.]. Nearshore currents and mean water elevation were modeled using the continuity equation together with the depth-averaged momentum equations. Sediment transport rates in the offshore and surf zone were computed using the sediment transport formulation proposed by Camenen and Larson [Camenen, B., Larson, M., 2005. A general formula for non-cohesive bed load sediment transport. Estuarine, Coastal and Shelf Science 63, 249-260.; Camenen, B., Larson, M., 2007. A unified sediment transport formulation for coastal inlet application. Technical report ERDC/CHL CR-07-1, US Army Engineer Research and Development Center, Vicksburg, MS.; Camenen, B., Larson, M., 2008. A general formula for non-cohesive suspended sediment transport. Journal of Coastal Research 24(3), 615-627.] together with the advection–diffusion equation, whereas the swash zone transport rate was obtained from the formulas derived by Larson and Wamsley [Larson, M., Wamsley, T.V., 2007. A formula for longshore sediment transport in the swash. Proceedings Coastal Sediments '07, ASCE, New Orleans, pp. 1924–1937.]. Three high-quality data sets from the LSTF experimental facility at the Coastal and Hydraulics Laboratory in Vicksburg, USA, were used to evaluate the predictive capability of the model. Good agreement between computations and measurements was obtained with regard to the cross-shore variation in waves, currents, mean water elevation, and sediment transport in the nearshore and swash zone. The present model will form the basis for predicting morphological evolution in the nearshore due to waves and currents with special focus on coastal structures.

1. Introduction

Accurate predictions of waves, nearshore currents, and sediment transport play a key role in solving coastal engineering problems, especially those related to beach morphological evolution. Waves and currents mobilize and transport sediment, and gradients in the transport cause deposition or erosion of sediment, affecting the local topography. Gradients in transport rate may occur naturally or be induced by man-made structures and activities such as groins, seawalls, detached breakwaters, dredging, and beach nourishment. In order to predict the beach morphological evolution for the purpose of engineering analysis and design, a robust model of nearshore waves, currents, and sediment transport is required.

There have been a number of studies on numerical modeling of nearshore waves, currents, and sediment transport (a brief review of relevant previous work is described in the next section). However, hydrodynamic and sediment transport processes are highly complex in the nearshore and swash zone, and presently there is no general model that yields robust and reliable predictions to be used in engineering studies for a wide range of conditions. Furthermore, the lack of high-quality and synchronized experimental data makes model validation difficult.

The overall objective of this study was to develop a robust and reliable numerical model of nearshore waves, currents, and sediment transport which can be applied in coastal engineering projects. First, the present paper discusses modifications of a multi-directional random wave transformation model (EBED), which was originally developed by Mase (2001), to improve the predictive capability of wave properties in the surf zone. Then, a model for nearshore currents due to random waves in the nearshore zone is developed. In order to make this model applicable for a

* Corresponding author. Department of Water Resources Engineering, Lund University, Box 118, S-22100, Lund, Sweden.
E-mail address: Thanh_Nam.Pham@tvrl.lth.se (P.T. Nam).

0378-3839/$ – see front matter © 2009 Elsevier B.V. All rights reserved.
doi:10.1016/j.coastaleng.2009.06.007

variety of conditions including complex alongshore bathymetry, a general depth-averaged two-dimensional model of the nearshore currents due to breaking waves and tides was formulated, although in this paper the focus is on the wave-induced currents. The two-dimensional creation and evolution of the surface roller in connection with wave breaking is modeled based on a period-averaged energy balance, as proposed by Dally and Osiecki (1994), Dally and Brown (1995), and Larson and Kraus (2002). Finally, a model to calculate the sediment transport in the nearshore zone, including the surf and swash zones, is developed based on the transport formulation by Camenen and Larson (2005, 2007, 2008), Larson and Wamsley (2007), and the advection–diffusion equation. The present model will subsequently form the basis for calculating beach topography change due to waves and currents.

The paper is structured as follows: Section 2 provides a brief review of previous work relevant to the present model development. In Section 3 the model description is given, including the four sub-models: (1) the wave model; (2) the surface roller model; (3) the nearshore wave-induced current model; and (4) the sediment transport model. Section 4 briefly describes the data sets employed from the Large-Scale Sediment Transport Facility (LSTF) basin of the Coastal and Hydraulics Laboratory (CHL), U.S. Army Engineer Research and Development Center (ERDC), in Vicksburg, United States. Section 5 summarizes the results of detailed model comparison with these data sets. Section 6 encompasses a discussion on various modeling results pertaining to the wave energy dissipation, surface roller and lateral mixing effects, bottom roughness height, suspended transport obtained by advection–diffusion equation, and sediment transport in swash zone. Finally, the conclusions are given in Section 7.

2. Review of relevant previous work

Waves in coastal areas display random characteristics; thus, random wave models are needed to properly assess the wave environment. Random wave transformation models can be classified into (i) phase-resolving models, and (ii) phase-averaging models. The first type of model, for example the ones based on the Boussinesq equations, is expressed through the conservation equations of mass and momentum (Madsen and Warren, 1984, Madsen et al., 1991, 1997; Nwogu, 1993). These models describe the main physical processes in the coastal area (e.g., shoaling, diffraction, refraction, and dissipation) at the intra-wave scale. Thus, they require fine resolution in space and time and, therefore, their applications are often only suitable for small coastal areas and short-term simulations. On the other hand, phase-averaging models, commonly based on the energy balance equation, describe slowly varying wave quantities (for example, wave amplitude and wave energy) on the scale of a wavelength. Thus, they can be applied for the prediction of multi-directional random wave transformation over large coastal areas. Originally, the non-stationary wave models WAM (WAMDI group, 1988) and SWAN (Booij et al., 1996) were based on phase-averaged equations including source terms. However, diffraction was not included in these models. Then, several attempts have been made in order to include diffraction effects in the phase-averaging wave model. For example, diffraction effects were included into the characteristic velocities through the wave number containing the second derivative of wave amplitude with respect to the spatial coordinates (Booij et al., 1997; Rivero et al., 1997; Holthuijsen et al., 2003). Although these models can be applied in the coastal zone containing structures, the numerical schemes seem to be unstable, especially for the discontinuities and singularities occurring (see Holthuijsen et al., 2003).

Mase (2001) developed a random wave transformation model called EBED in which diffraction effect was included. The diffraction term was derived from a parabolic approximation of the wave equation. The numerical scheme is stable and the model can be applied for complex coastal areas with structures. In the present study, the EBED model was employed to calculate wave transformation after modifications to more accurately predict the wave conditions in the surf zone. Although, structures were not included in the investigated data of this study, the long-term objective is to model the hydrodynamics and morphological evolution in the vicinity of structures. Therefore, it is necessary to employ a wave model that includes diffraction.

There have been a number of numerical models for wave-driven currents after the concept of radiation stress was introduced by Longuet-Higgins and Stewart (1964). Early simulations of longshore current induced by regular waves, for a simple plan form beach, were carried out by Bowen (1969), Longuet-Higgins (1970), and Thornton (1970). The disadvantage of these semi-analytic models is the occurrence of an abrupt change in longshore current at the break point. By introducing an eddy viscosity term (i.e., lateral mixing) in the momentum equation for the longshore current, the physically unrealistic current distribution at the breaker-line was eliminated. Since the early models, significant progress has been made concerning nearshore currents generated by random waves. The pioneering work of Battjes (1972) illustrated that the longshore current generated by random waves is smooth in the surf zone, even though the lateral mixing term is not included. Thornton and Guza (1986) presented a model for the longshore current based on their random wave breaking model (Thornton and Guza, 1983). Van Dongeren et al. (1994, 2003), and Van Dongeren and Svendsen (2000) developed a quasi-3D nearshore hydrodynamic model named SHORECIRC, which is capable of describing several phenomena such as the edge waves, surf beats, infragravity waves, and longshore current. Kraus and Larson (1991), Larson and Kraus (2002) developed the NMLong model for computing the longshore current focusing on barred beaches. Militello et al. (2004) developed the M2D model for simulating the nearshore current due to tide, waves, wind, and rivers. Recently, Goda (2006) examined the influence of several factors on the longshore current under random waves. He demonstrated that significant differences in wave height and longshore velocity resulted depending on the employed random wave breaking model. Thus, selecting a wave model that can accurately simulate surf-zone conditions is important when computing wave-induced nearshore currents.

Much research has demonstrated that the surface roller plays an important role in generating nearshore currents. The roller was initially investigated in the laboratory by Duncan (1981) and first applied theoretically by Svendsen (1984a,b) to improve the modeling of wave setup and undertow in the surf zone. Then, the roller model, including the roller energy gradients in the energy flux balance based on the roller theory of Svendsen (1984a,b), was employed in many studies related to wave-induced currents (e.g. Nairn et al., 1990; Deigaard et al., 1991; Stive and De Vriend, 1994; Lippmann et al., 1996; Reniers and Battjes, 1997; Ruessink et al., 2001). Van Dongeren et al. (2003) extended the roller energy flux balance equation derived by Nairn et al. (1990), and they obtained calculations of longshore current that were in good agreement with the data from the DELILAH field experiment. Based on the depth-integrated and period-averaged energy balance equation, Dally and Osiecki (1994), and Dally and Brown (1995) developed a roller model for the evolution of the roller itself. Larson and Kraus (2002) applied this model in NMLong to improve longshore current simulations. In the energy balance equation, the energy dissipation per unit area after Dally et al. (1985) was used instead of the gradient in the depth-integrated time-averaged wave-induced energy flux in the x-direction. In general, the roller energy flux is only considered in the cross-shore direction in the balance equation. In the present study, the approaches by Dally and Brown (1995) and Larson and Kraus (2002) were followed, and the energy flux term in alongshore direction was included in the energy balance equation for the evolution of the roller itself.

Calculating sediment transport in the nearshore zone is a challenge because of the complexity of the hydrodynamics and the variety of governing phenomena. There are a number of nearshore sediment transport formulas that have been developed through the years for different types of applications in coastal engineering. For example, several formulas were examined and evaluated by Bayram et al. (2001), and Camenen and Larroude (2003). However, these formulas

have typically described a specific set of physical processes and been validated with limited data. Recently, Camenen and Larson (2005, 2007, 2008) developed a unified sediment transport formulation, which has been validated for a large set data on longshore and cross-shore sediment transport from the laboratory and field. Performance of the new sediment transport formulation was compared to several popular existing formulas, and the new formulation yielded the overall best predictions among investigated formulations, and therefore, it was employed in this study.

The mechanics of sediment transport in the swash zone have received less attention than the surf zone. However, the swash zone is important for the sediment exchange between land and sea, which in turn affects both the sub-aerial and sub-aquaeous evolution of the beach. The limited number of studies, as well as lack of measurement data on net transport in the swash, has made it difficult to formulate mathematical models based on a detailed understanding of the governing physics. In spite of these difficulties, significant progress has been made in the last decade concerning the hydrodynamics and sediment transport conditions in the swash zone (see Elfrink and Baldock, 2002; Larson et al., 2004; Larson and Wamsley, 2007). In this study, the formulas of hydrodynamics and sediment transport rates in swash zone of Larson and Wamsley (2007) were employed. The obtained sediment transport rate at the still-water shoreline was used as boundary condition for computing the suspended load in the inner surf zone, which was derived from the advection–diffusion equation.

3. Model description

3.1. Wave model

3.1.1. The random wave model EBED

Mase (2001) developed a multi-directional random wave transformation model based on the energy balance equation with energy dissipation and diffraction terms (EBED). The governing equation, for steady state, is expressed as follows,

$$\frac{\partial(v_x S)}{\partial x}+\frac{\partial(v_y S)}{\partial y}+\frac{\partial(v_\theta S)}{\partial \theta}=\frac{\kappa}{2\omega}\left\{(CC_g\cos^2\theta S_y)_y-\frac{1}{2}CC_g\cos^2\theta S_{yy}\right\}-\varepsilon_b S \tag{1}$$

where S is the angular-frequency spectrum density, (x, y) are the horizontal coordinates, θ is the angle measured counterclockwise from the x axis, ω is the frequency, C is the phase speed, and C_g the group speed, (v_x, v_y, v_θ) are the propagation velocities given by,

$$(v_x, v_y, v_\theta)=\left(C_g\cos\theta, C_g\sin\theta, \frac{C_g}{C}\left(\sin\theta\frac{\partial C}{\partial x}-\cos\theta\frac{\partial C}{\partial y}\right)\right) \tag{2}$$

The first term on the right-hand side is added in the balance equation in order to represent the diffraction effects, and κ is a free parameter that can be optimized to change the influence of the diffraction effects. The second term represents the wave energy dissipation due to wave breaking, and ε_b is the energy dissipation coefficient. The output from the wave transformation model includes three main wave parameters: significant wave height H_s, significant wave period T_s, and mean wave direction $\bar{\theta}$.

3.1.2. The modified-EBED model

The original EBED model is stable and can be applied to the complex beach topography of coastal zones containing structures. However, the obtained output from the model often overestimates the wave parameters in the surf zone compared to measurements. The overestimation is due mainly to the algorithm describing wave energy dissipation caused by wave breaking. In the EBED model, the energy dissipation coefficient was determined by the Takayama et al. (1991) model. The calculation of this coefficient is rather complex and the coefficient does not easily lend itself to calibration.

In this study, a new approach for calculating the energy dissipation term, which was based on the Dally et al. (1985) model, was employed for improving the predictive capability of the wave model. The model is referred to as the Modified-EBED model in this paper hereafter. Thus, a modified energy balance equation is proposed as follows,

$$\frac{\partial(v_x S)}{\partial x}+\frac{\partial(v_y S)}{\partial y}+\frac{\partial(v_\theta S)}{\partial \theta}=\frac{\kappa}{2\omega}\left\{(CC_g\cos^2\theta S_y)_y-\frac{1}{2}CC_g\cos^2\theta S_{yy}\right\}-\frac{K}{h}C_g(S-S_{stab}) \tag{3}$$

where h is the still-water depth, K is dimensionless decay coefficient, S_{stab} is the stable wave spectrum density, which is determined based upon the stable wave height H_{stab} ($=\Gamma h$), with Γ being a dimensionless empirical coefficient.

Assuming that the spectrum density S and the stable spectrum density S_{stab} are functions of H_s^2 and H_{stab}^2, respectively, the dissipation term in Eq. (3) can be rewritten as,

$$D_{diss}=\frac{K}{h}C_g S\left[1-\left(\frac{\Gamma h}{H_s}\right)^2\right]. \tag{4}$$

In the Dally et al. (1985) model, the recommended values for Γ and K were 0.4 and 0.15, respectively. Goda (2006) used his formula in 1975 for determining the decay coefficient, $K=3(0.3+2.4\,s)/8$, where s is the bottom slope. In the Modified-EBED model, in order to obtain a good description of wave conditions in the surf zone for the LSTF data, the coefficients were modified according to:

$$\begin{cases}\Gamma=0.45, K=\dfrac{3}{8}(0.3-19.2s) & : s<0\\ \Gamma=0.45+1.5s, K=\dfrac{3}{8}(0.3-0.5s) & : s\geq 0\end{cases}. \tag{5}$$

The wave radiation-driven stresses were determined by the output from the wave model,

$$S_{xx}=\frac{E}{2}[2n(1+\cos^2\bar{\theta})-1] \tag{6}$$

$$S_{yy}=\frac{E}{2}[2n(1+\sin^2\bar{\theta})-1] \tag{7}$$

$$S_{xy}=S_{yx}=\frac{E}{2}n\sin 2\bar{\theta} \tag{8}$$

where $E=\rho g H_{rms}^2/8$ is the wave energy per unit area, and $n=C_g/C$ is the wave index.

3.2. Surface roller model

The wave energy balance equation for the surface roller in two dimensions is expressed as (Dally and Brown, 1995; Larson and Kraus, 2002),

$$P_D+\frac{\partial}{\partial x}\left(\frac{1}{2}MC_r^2\cos^2\bar{\theta}\right)+\frac{\partial}{\partial y}\left(\frac{1}{2}MC_r^2\sin^2\bar{\theta}\right)=g\beta_D M \tag{9}$$

where P_D is the wave energy dissipation ($=KC_g\rho g(H_{rms}^2-(\Gamma h))^2)/(8h)$), M is the wave-period-averaged mass flux, C_r is the roller speed ($\approx C$), and β_D is the roller dissipation coefficient.

The stresses due to the rollers are determined as follows:

$$R_{xx}=MC_r\cos^2\bar{\theta} \tag{10}$$

$$R_{yy} = MC_r \sin^2 \bar{\theta} \tag{11}$$

$$R_{xy} = R_{yx} = MC_r \sin 2\bar{\theta}. \tag{12}$$

3.3. Nearshore current model

The governing equations for the nearshore currents are written as (Militello et al., 2004),

$$\frac{\partial(h+\eta)}{\partial t} + \frac{\partial q_x}{\partial x} + \frac{\partial q_y}{\partial y} = 0 \tag{13}$$

$$\frac{\partial q_x}{\partial t} + \frac{\partial u q_x}{\partial x} + \frac{\partial v q_x}{\partial y} + g(h+\eta)\frac{\partial \eta}{\partial x} = \frac{\partial}{\partial x} D_x \frac{\partial q_x}{\partial x} + \frac{\partial}{\partial y} D_y \frac{\partial q_x}{\partial y} + f q_y - \tau_{bx} + \tau_{Sx} \tag{14}$$

$$\frac{\partial q_y}{\partial t} + \frac{\partial u q_y}{\partial x} + \frac{\partial v q_y}{\partial y} + g(h+\eta)\frac{\partial \eta}{\partial y} = \frac{\partial}{\partial x} D_x \frac{\partial q_y}{\partial x} + \frac{\partial}{\partial y} D_y \frac{\partial q_y}{\partial y} - f q_x - \tau_{by} + \tau_{Sy} \tag{15}$$

where η is the water elevation, q_x,q_y is the flow per unit width parallel to the x and y axis, respectively, u,v is the depth-averaged velocity in x and y direction, respectively, g is the acceleration due to gravity, D_x,D_y are the eddy viscosity coefficients, f is the Coriolis parameter, τ_{bx},τ_{by} are the bottom stresses, and τ_{Sx},τ_{Sy} are the wave stresses (the latter variables are all in the x and y directions, respectively).

The depth-averaged horizontal eddy viscosity coefficient can be calculated as a function of the total water depth, current speed, and bottom roughness according to Falconer (1980),

$$D_0 = 1.154 g(h+\eta)\frac{|U|}{C_z^2} \tag{16}$$

where C_z is the Chezy roughness coefficient.

In the surf zone, the eddy viscosity is simulated as a function of the wave properties,

$$D_1 = \varepsilon_L \tag{17}$$

where ε_L represent the lateral mixing below the trough level. Kraus and Larson (1991) expressed this term as,

$$\varepsilon_L = \Lambda u_m H_{rms} \tag{18}$$

in which H_{rms} is the root-mean-square wave height, Λ is an empirical coefficient, and u_m is the wave orbital velocity at the bottom.

In the transition zone, the eddy viscosity is calculated as,

$$D_2 = (1-\alpha)D_0 + \alpha D_1 \tag{19}$$

where α is weighting parameter ($=(H_{rms}/(h+\eta))^3$, see Militello et al., 2004).

The bottom stresses under combined current and waves are determined from Nishimura (1988),

$$\tau_{bx} = C_b\left[\left(U_{wc} + \frac{\omega_b^2}{U_{wc}}\cos^2\bar{\theta}\right)u + \left(\frac{\omega_b^2}{U_{wc}}\cos\bar{\theta}\sin\bar{\theta}\right)v\right] \tag{20}$$

$$\tau_{by} = C_b\left[\left(U_{wc} + \frac{\omega_b^2}{U_{wc}}\sin^2\bar{\theta}\right)v + \left(\frac{\omega_b^2}{U_{wc}}\cos\bar{\theta}\sin\bar{\theta}\right)u\right] \tag{21}$$

in which C_b is the bottom friction coefficient, U_{wc}, and ω_b are given by,

$$U_{wc} = \frac{1}{2}\left\{\sqrt{|u^2+v^2+\omega_b^2+2(u\cos\bar{\theta}+v\sin\bar{\theta})\omega_b|} + \sqrt{|u^2+v^2+\omega_b^2-2(u\cos\bar{\theta}+v\sin\bar{\theta})\omega_b|}\right\} \tag{22}$$

$$\omega_b = \frac{\sigma H_{rms}}{\pi \sinh[k(h+\eta)]} \tag{23}$$

where σ is the wave frequency, and k the wave number.

The wave stresses are derived from the wave transformation model and the surface roller model. They are expressed by the following formulas:

$$\tau_{Sx} = -\frac{1}{\rho_w}\left[\frac{\partial}{\partial x}(S_{xx}+R_{xx}) + \frac{\partial}{\partial y}(S_{xy}+R_{xy})\right] \tag{24}$$

$$\tau_{Sy} = -\frac{1}{\rho_w}\left[\frac{\partial}{\partial x}(S_{xy}+R_{xy}) + \frac{\partial}{\partial y}(S_{yy}+R_{yy})\right]. \tag{25}$$

3.4. Sediment transport

3.4.1. Swash zone

Larson and Wamsley (2007) developed the formula for the net transport rates in the cross-shore and longshore direction, respectively, as,

$$q_{bc,net} = K_c \frac{\tan\phi_m}{\tan^2\phi_m - (dh/dx)^2}\frac{u_0^3}{g}\left(\frac{dh}{dx} - \tan\beta_e\right)\frac{t_0}{T} \tag{26}$$

$$q_{bl,net} = K_l \frac{\tan\phi_m}{\tan^2\phi_m - (dh/dx)^2}\frac{u_0^2 v_0}{g}\frac{t_0}{T} \tag{27}$$

where $q_{bc,net}$, $q_{bl,net}$ are the net transport in the cross-shore and longshore direction, respectively, K_c and K_l are empirical coefficients, ϕ_m the friction angle for a moving grain ($\approx 30°$), β_e the foreshore equilibrium slope, u_0,v_0 and t_0 the scaling velocities and time, respectively, and T the swash duration (assumed that T is equal to the incident wave period). The swash zone hydrodynamics without friction, which were derived based on the ballistic theory, were employed in the model (for details see Larson and Wamsley, 2007).

3.4.2. Nearshore zone (offshore and surf zone)

Camenen and Larson (2005, 2007, 2008) developed a general transport formulation for bed load and suspended load under combined waves and current. It is referred as the Lund-CIRP formula in this paper hereafter. It can be used for both sinusoidal and asymmetric waves. To simplify calculations, the waves are assumed to be sinusoidal, having no asymmetry. Thus, the contribution to the transporting velocity from waves is negligible, implying that only the current moves the material. In such case, the bed load transport can be expressed as,

$$\frac{q_{bc}}{\sqrt{(s-1)g d_{50}^3}} = a_c\sqrt{\theta_c}\theta_{cw,m}\exp\left(-b_c\frac{\theta_{cr}}{\theta_{cw}}\right) \tag{28}$$

where the transport q_{bc} is obtained in the direction of the current, the transport normal to the current is zero, s is the relative density between sediment and water, d_{50} is the median grain size, a_c and b_c are empirical coefficients, $\theta_{cw,m}$ and θ_{cw} are the mean and maximum Shields parameters due to wave and current interaction, respectively, θ_{cr} is the critical Shields parameter, and θ_c is the Shields parameter due to current.

The suspended load is calculated based on the assumption of an exponential concentration profile and a constant velocity over the water column,

$$q_s = U_c c_R \frac{\varepsilon}{w_s}\left[1-\exp\left(-\frac{w_s d}{\varepsilon}\right)\right] \tag{29}$$

where U_c is current velocity, c_R is the reference concentration at the bottom, w_s is the sediment fall speed, ε is the sediment diffusivity, and d is the total depth $(=h+\eta)$.

The bed reference concentration is obtained from,

$$c_R = A_{cR}\theta_{cw,m}\exp\left(-4.5\frac{\theta_{cr}}{\theta_{cw}}\right) \tag{30}$$

where the coefficient A_{cR} is written as,

$$A_{cR} = 3.5\,10^{-3}\exp(-0.3d_*) \tag{31}$$

with $d_* = \sqrt[3]{(s-1)g/\upsilon^2}\,d_{50}$ being the dimensionless grain size and υ is the kinematic viscosity of water.

The sediment fall speed is determined from Soulsby (1997) as:

$$w_s = \frac{\upsilon}{d_{50}}\left[\left(10.36^2 + 1.049d_*^3\right)^{1/2} - 10.36\right]. \tag{32}$$

The sediment diffusivity is related to the energy dissipation as (Battjes, 1975; Camenen and Larson, 2008),

$$\varepsilon = \left(\frac{k_b^3 D_b + k_c^3 D_c + k_w^3 D_w}{\rho}\right)^{1/3} d \tag{33}$$

where the energy dissipation from wave breaking (D_b) and from bottom friction due to current (D_c) and waves (D_w) were simply added, and k_b, k_c and k_w are coefficients (see Camenen and Larson, 2008).

Alternatively, the suspended load can be obtained by solving the advection–diffusion equation. The advection–diffusion equation is obtained from the continuity of depth-averaged suspended sediment transport as,

$$\frac{\partial(\overline{C}d)}{\partial t} + \frac{\partial(\overline{C}q_x)}{\partial x} + \frac{\partial(\overline{C}q_y)}{\partial y} = \frac{\partial}{\partial x}\left(K_x d\frac{\partial\overline{C}}{\partial x}\right) + \frac{\partial}{\partial x}\left(K_y d\frac{\partial\overline{C}}{\partial y}\right) + P - D \tag{34}$$

where $\bar{C}$ is the depth-averaged sediment concentration, K_x and K_y are the sediment diffusion coefficient in x and y direction, respectively, P is the sediment pick-up rate, and D is the sediment deposition rate.

The sediment diffusion coefficient can be calculated by Elder (1959) as,

$$K_x = K_y = 5.93u_{*c}d \tag{35}$$

where u_{*c} is shear velocity from the current only.

The sediment pick-up and deposition rates, respectively, are obtained as,

$$P = c_R w_s \tag{36}$$

$$D = \frac{\overline{C}}{\beta_d}w_s \tag{37}$$

where β_d is a coefficient calculated based on Camenen and Larson (2008); see also Militello et al., 2006),

$$\beta_d = \frac{\varepsilon}{w_s d}\left[1-\exp\left(-\frac{w_s d}{\varepsilon}\right)\right]. \tag{38}$$

The suspended transport rates in the x and y directions can be calculated from Eq. (34) as:

$$q_{sx} = \overline{C}q_x - K_x d\frac{\partial\overline{C}}{\partial x} \tag{39}$$

$$q_{sy} = \overline{C}q_y - K_y d\frac{\partial\overline{C}}{\partial y}. \tag{40}$$

The sediment transport rate is often large near the shoreline because of swash uprush and backwash processes. For example, the measurements from LSTF showed a peak in the sediment transport rate close to the shoreline that was larger than in the inner surf zone. The computed sediment transport rates obtained from currently available formulas often tend to decrease too rapidly from the swash zone towards the offshore. Thus, the interaction between the swash zone and the inner part of the surf zone is not well described. Therefore, the calculations of sediment transport may not agree with measurements in this region, unless some modifications are introduced.

In the present study, we use the sediment transport at the still-water shoreline obtained from swash zone computations as the boundary value for computing suspended load in the surf zone using the advection–diffusion equation. Furthermore, the pick-up and deposition rates described in the Eqs. (36) and (37), respectively, were also modified as follows,

$$\tilde{P} = P\left[1 + \vartheta\frac{\overline{V}}{v_0}\exp\left(-\mu\frac{d}{R}\right)\right] \tag{41}$$

$$\tilde{D} = \frac{D}{\left[1 + \vartheta\frac{\overline{V}}{v_0}\exp\left(-\mu\frac{d}{R}\right)\right]} \tag{42}$$

where ϑ and μ are free non-negative coefficients, $\overline{V}$ is the mean velocity across the profile, R is the runup height. The velocity $\overline{V}$ is determined as the average longshore current across the surf zone, v_0 is obtained from swash zone computation, and R is calculated by the Hunt (1959) formula.

The total load, given by the bed load from the Lund-CIRP formula and the suspended load calculated by the advection–diffusion equation with the above modifications, is referred to as AD-Lund-CIRP hereafter. The above modifications increase the suspended sediment load near the shoreline. The empirical parameter values introduced are related to the magnitude of longshore current, scaling velocity, water depth, and runup height. Although the modifications are somewhat ad hoc, the model produces more reasonable computed sediment fluxes in agreement with the investigated measured data.

4. Large-Scale Sediment Transport Facility (LSTF) data

Five series of movable bed physical model experiments were carried out in the LSTF basin (see Hamilton and Ebersole, 2001; Wang et al., 2002) at the Coastal and Hydraulics Laboratory of the U.S. Army Engineer Research and Development Center in Vicksburg, Mississippi by Gravens and Wang (2007), and Gravens et al. (2006). The first series of experiments, referred to as "Base Cases", including four runs of approximately 160 min each on a natural beach (without structure), were aimed at generating high-quality data sets for testing and validation of sand transport formulas due to waves and currents. The

Table 1.
Measurement locations for LSTF Base Cases.

Measured locations	ADV1	ADV2	ADV3	ADV4	ADV5	ADV6	ADV7	ADV8	ADV9	ADV10
Distance to shoreline (m)	1.125	2.725	4.125	5.73	7.125	8.525	10.125	11.625	13.125	15.625

four remaining series of experiments were designed to generate data sets for testing and validation of the development of tombolos in the lee of nearshore detached breakwaters and T-head groins. Spilling breaking waves were generated by four wave generators. The beach consisted of very well-sorted fine quartz sand with a median grain size of 0.15 mm. The longshore current generated by the obliquely incident waves was circulated with twenty turbine pumps through twenty flow channels at the updrift and downdrift ends of the basin.

In this study, the Base Cases were used for validation of the model. In Base Case 1 (BC-1) the longshore current was induced by random waves and circulated by the turbine pumps. Base Case 2 (BC-2) encompassed the wave-induced current and an external longshore current which was generated by recirculating two times the wave-generated longshore flux of water. In Base Case 3 (BC-3) the wave generators were not operated so it was not used for testing the numerical model. Similar to BC-2, the external longshore current was also imposed across the model beach in Base Case 4 (BC-4) by recirculating 1.5 times the wave-generated longshore flux of water. The wave height, wave period, and wave setup were measured by thirteen capacitance gauges. However, the wave sensor at ADV10 did not work so the measured data on wave conditions at this location was not available. The data on nearshore current were collected and measured by ten Acoustic Doppler Velocimeters (ADVs). Ten wave and current sensors were collocated at ten cross-shore locations and synchronized in time for each of the eleven cross-shore sections. These locations are presented in Table 1. The remaining wave sensors, Gauge#11, Gauge#12 and Gauge#13, were located at three alongshore positions, 18.43 m seaward from the still-water shoreline, to measure wave conditions outside the toe of the movable beach (see Fig. 1). Twenty-one gravity-feed sediment traps located at the downdrift end of the movable bed model beach, in which two traps were located in the swash zone, were used to measure the magnitude and cross-shore distribution of sand transport. Beach profiles at the interval between 0.25 and 4 m were measured by rod and acoustic survey techniques after each model run.

5. Model simulation results

The computational grid for the LSTF beach was generated based on interpolation of measured beach profile data from profile Y34 to profile Y14 (see Fig. 1). The grid size was 0.2×0.2 m, and the measurements at Gauge#11, Gauge#12, and Gauge#13 were used as offshore wave conditions. The detailed information of the wave conditions at these points for cases BC-1, BC-2, and BC-4 are presented in Table 2. A TMA spectrum was assumed at the offshore boundary with the parameter values $\gamma = 3.3$, $\sigma_a = 0.07$, $\sigma_b = 0.09$, and $S_{max} = 25$. Values for the decay and stable coefficients were determined from Eq. (5). Because the beach topography of the Base Cases is fairly uniform in the alongshore direction, the variation in alongshore significant wave height and longshore current was relative small. Therefore, the comparisons between calculation and measurement in this paper were only made at the profile Y24 (center profile).

Fig. 2 shows the comparison between calculated and measured significant wave height for case BC-1. The dashed line is the calculated significant wave height obtained by the original EBED model, which overestimated the wave height in the surf zone compared to the measured data. By employing the new method for calculating wave energy dissipation due to breaking, the Modified-EBED model produced improved results. The calculated significant wave height agreed well with the measured data at all measurement locations. The root-mean-square (rms) error of the significant wave height obtained by Modified-EBED model was only 3.6%, whereas it was 13.0% for the EBED model.

The output from the Modified-EBED model, such as significant wave height, wave direction, and wave period, as well as wave-driven stresses, were employed to calculate the nearshore currents. The

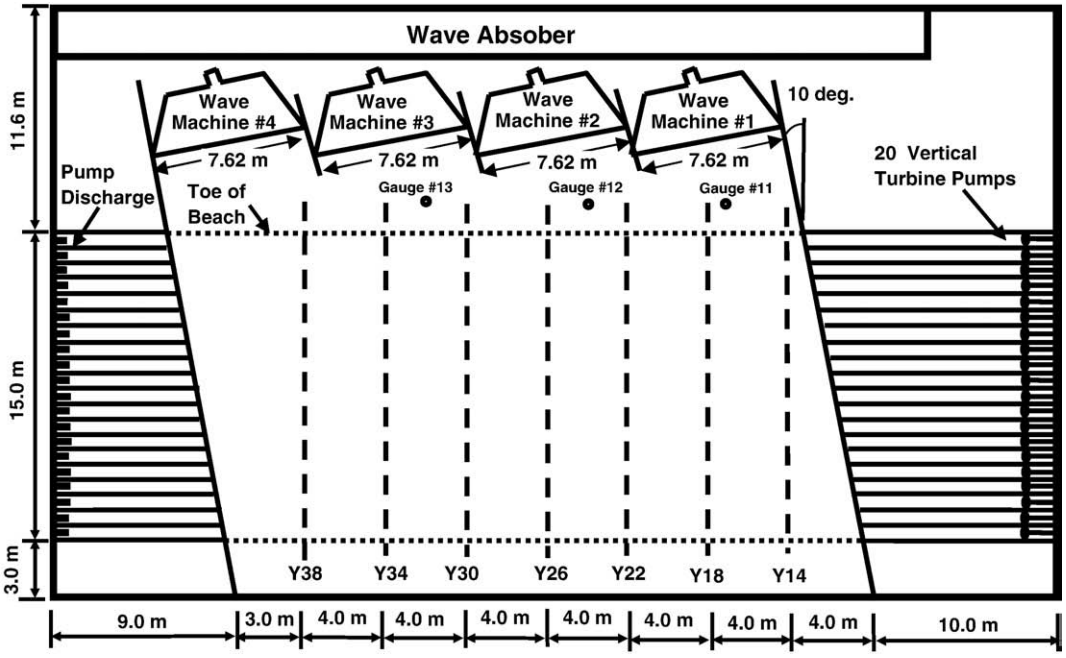

Fig. 1. Configuration of LSTF basin (Gravens and Wang, 2007).

Table 2
Offshore wave conditions for LSTF Base Cases.

Data sets	Gauges	H_{mo} (m)	T_p (s)	Θ (°)
BC-1	#11	0.220	1.444	6.5
	#12	0.225	1.468	6.5
	#13	0.228	1.465	6.5
BC-2	#11	0.213	1.439	6.5
	#12	0.226	1.469	6.5
	#13	0.228	1.460	6.5
BC-4	#11	0.216	1.447	6.5
	#12	0.221	1.472	6.5
	#13	0.222	1.460	6.5

Chezy coefficient was specified to be 40, the coefficient for lateral mixing $\Lambda = 0.5$, the roller dissipation coefficient $\beta_D = 0.1$, and the time step 0.02 s. The water fluxes on the upstream boundary were given based on measured data on longshore current at profile Y34. The downstream boundary was treated as an open boundary.

Fig. 3 illustrates the measurement data and computations of the wave-induced longshore current with and without roller. The roller effects did not only cause a shift in the longshore current towards the shoreline but also increased the maximum current in the surf zone. Although there were differences between measured and calculated longshore current with the roller at ADV3 and ADV4, the tendency after including the roller is to improve the agreement with measured data in the surf zone. The rms errors of the calculated longshore current with and without roller were 27.2% and 29.8%, respectively.

The comparison of calculated and measured wave setup is presented in Fig. 4. Both calculations of wave setup with and without roller agree well with the measurements. The setup without roller yielded slightly better agreement with the measurements compared to the setup with roller. Although the rms error of wave setup with roller (32.5%) was higher than without roller (24.3%), the difference between the computations was relatively small.

In order to calculate the scaling velocities, the runup height and wave angle prior to runup are needed. The runup height was determined by the Hunt (1959) formula. The wave angle prior to runup was given by the wave angle at the cell next to the shoreline from the Modified-EBED model output. The foreshore equilibrium slope was determined based on the observed topographical data. The values of K_c and K_f were both set to 0.0008, following Larson and Wamsley (2007).

The computed longshore sediment flux in the swash zone is presented by the dashed line in Fig. 5. There were only two measurement points in the swash zone, but the calculated longshore sediment flux is in good agreement with the measured data.

The output from the Modified-EBED model and the nearshore wave-induced currents with roller were used to determine the Shields parameters due to waves and currents. The kinematic viscosity of water υ was set to 1.36×10^{-6} m^2/s, and the density of water and sediment was given as 1000 kg/m^3 and 2650 kg/m^3, respectively. The critical Shields parameter was determined by the Soulsby and Whitehouse formula (see Soulsby, 1997). The coefficient values in the bedload transport formula a_c and b_c were given as 12 and 4.5, respectively (see Camenen and Larson, 2005). In the suspended load formula, a value of $k_b = 0.017$ was employed and k_c and k_w were calculated based on the Schmidt number (see Camenen and Larson, 2008). The coefficient values $\vartheta = 9.3$ and $\mu = 2.4$ were employed for calculating the pick-up and deposition rates. In addition, the total load formula of Watanabe (1987) with a transport coefficient equal to 1.0 was employed to compare with the Lund-CIRP and AD-Lund-CIRP.

The computations of the longshore sediment flux in the nearshore are presented in Fig. 5. There was only a slight difference in the longshore sediment flux between the Lund-CIRP and Watanabe formulas, and these calculations agree fairly well with the measured data in the offshore and outer surf zone. However, there is a significant difference between measurements and computations near the shoreline for these two formulas. Using AD-Lund-CIRP overcomes this discrepancy. Based on the calculations of longshore sediment flux in the swash zone and the modifications of pick-up and deposition rates in the advection–diffusion equation, the computed longshore sediment flux in the inner part of the surf zone also agrees with the measurements. The rms error of longshore sediment flux obtained by AD-Lund-CIRP for both swash zone and nearshore zone was 33.2%, better than those by Lund-CIRP (49.1%) and by Watanabe (49.6%).

The computations of waves, nearshore current, and sediment transport for BC-2 and BC-4 were carried out in the same manner as for BC-1. The coefficient values used for BC-1 were kept the same in the simulations for BC-2 and BC-4.

The significant wave height, longshore current, wave setup, and longshore sediment flux for BC-2 were presented in Figs. 6–9, respectively. As for BC-1, the wave predictions by the Modified-EBED model were better than those by the EBED model agreeing well with the measured data. The longshore current and wave setup were also well predicted (including roller effects). Although the overall shape of cross-shore distribution of the longshore current was in good agreement with the data, the magnitude of the current at ADV3 and ADV4 was overestimated. Sediment transport rate in the swash zone agreed well with the measured data. The difference between longshore sediment flux obtained by Lund-CIRP and Watanabe was more pronounced in the surf zone than for BC-1, especially between 0.2 m and 5.6 m seaward of the still-water shoreline. However, computations

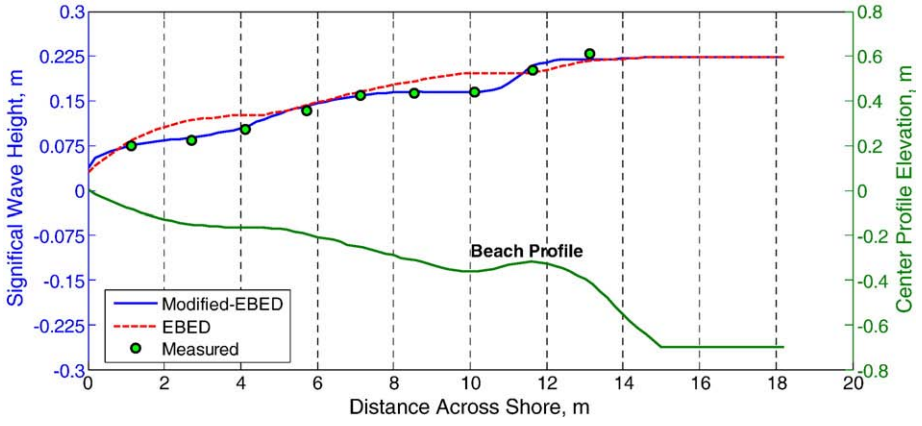

Fig. 2. Computed and measured significant wave height for LSTF BC-1.

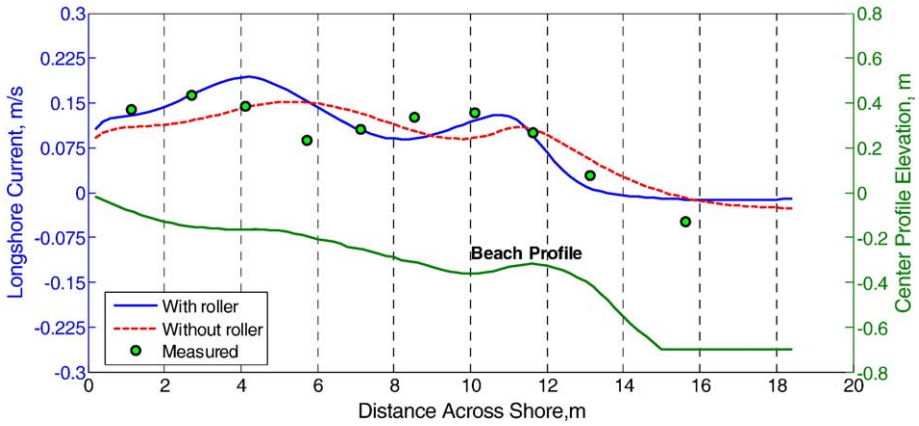

Fig. 3. Computed and measured longshore current for LSTF BC-1.

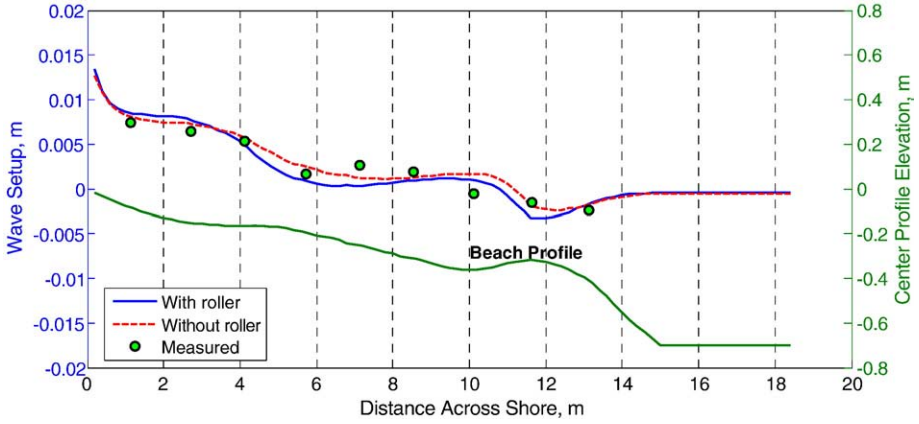

Fig. 4. Computed and measured wave setup for LSTF BC-1.

with both Lund-CIRP and Watanabe showed the same tendency of decreasing sediment flux towards the shoreline as for BC-1. Calculation with AD-Lund-CIRP, including the swash zone computation, produced reasonable sediment fluxes from the swash zone to the offshore.

Computational results and comparison with measurements for BC-4 regarding significant wave height, longshore current, wave setup, and longshore sediment flux were presented in Figs. 10–13, respectively. The significant wave height obtained by Modified-EBED agreed well with the measured data, except at ADV3 and ADV4, and the nearshore current model produced satisfactory predictions of the longshore current. However, in this run, the measured wave setup at ADV1, ADV2, ADV3, and ADV4 were too small compared to the calculated results, especially at ADV3 and ADV4 where wave setdown was observed. The mean water elevation should normally increase in the surf zone for a monotonically increasing profile, similar to what was observed in BC-1 and BC-2, so the data may contain some errors at these gauges. From ADV5 to ADV10, the calculated wave setup agrees well with the measured data. The computed longshore sediment fluxes were not as good as for BC-1 and BC-2. It was difficult to obtain good agreement between calculated and measured sediment flux in the inner surf zone near the shoreline, but AD-Lund-CIRP gave the best predictions of the longshore sediment flux compared to the Lund-CIRP and Watanabe formulas.

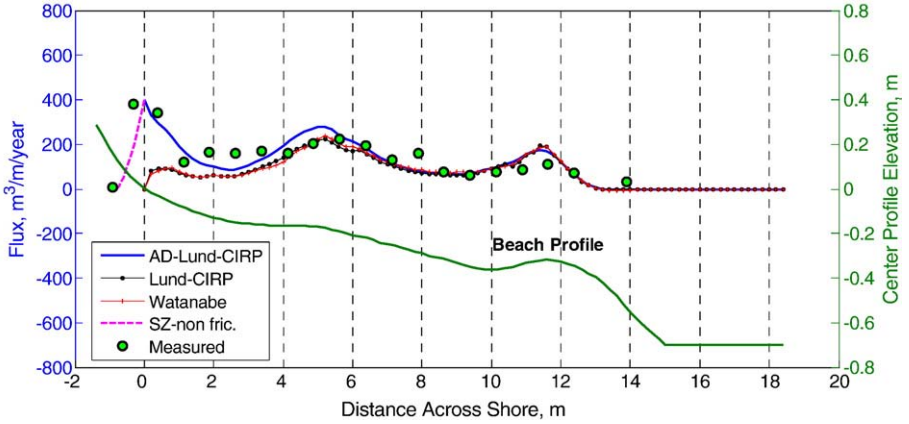

Fig. 5. Computed and measured longshore sediment flux for LSTF BC-1.

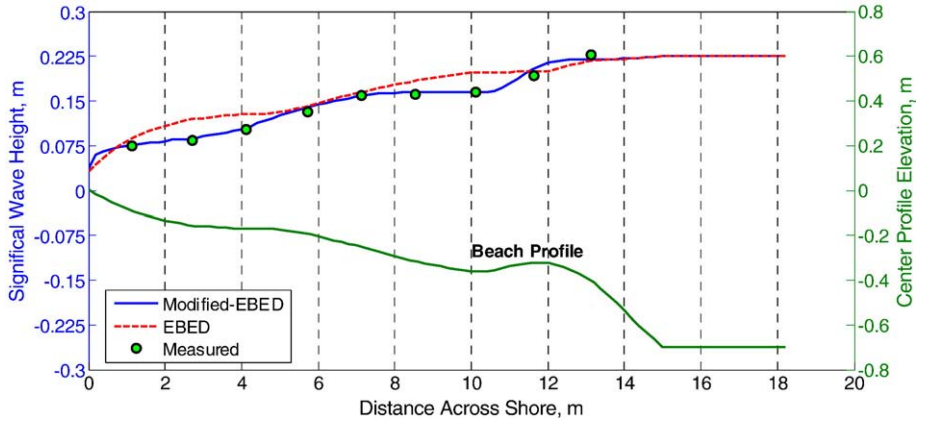

Fig. 6. Computed and measured significant wave height for LSTF BC-2.

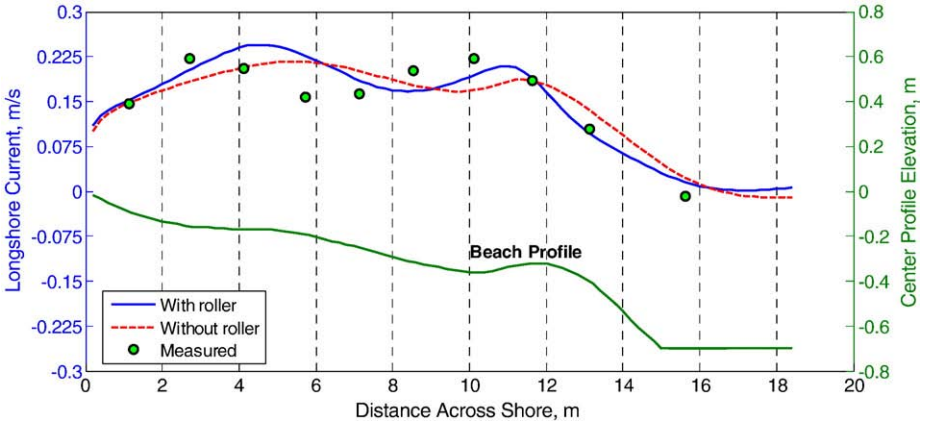

Fig. 7. Computed and measured longshore current for LSTF BC-2.

A quantitative assessment of the predictive capacity of the model was performed based on the rms error. Table 3 summarizes in detail the rms errors between computations and measurements for significant wave height obtained by the Modified-EBED and EBED model, and for the longshore current and wave setup with and without roller. Table 4 presents the quantitative assessment of the longshore sediment transport calculations in both the nearshore and the swash zone. The assessment showed that the developed model can produce reasonable computational results for the investigated data sets.

6. Discussion

In the neashore zone, energy dissipation due to wave breaking is an important process to describe in the wave model. The Takayama approach used in the original EBED model often caused an over-estimation of the wave heights in the surf zone. Thus, the modification of the energy dissipation calculations in the EBED model following Dally et al. (1985) implied a significant improvement in computing waves in the surf zone. However, appropriate values on the decay and stable coefficients should be given. The coefficient values determined

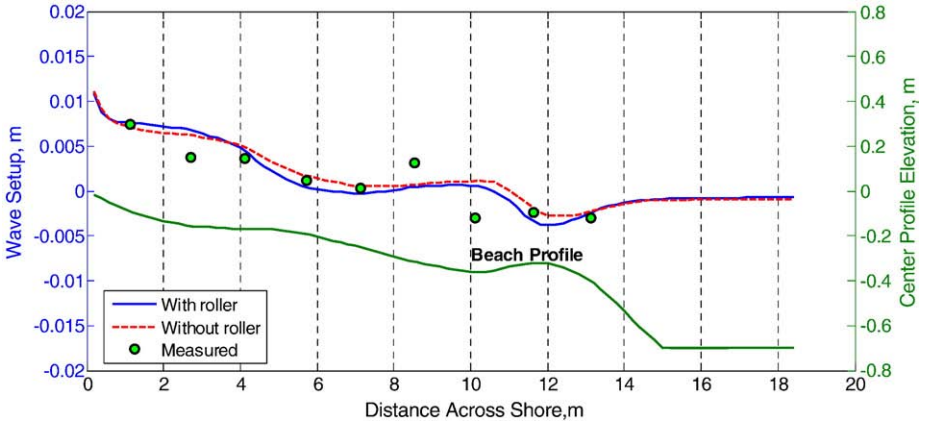

Fig. 8. Computed and measured wave setup for LSTF BC-2.

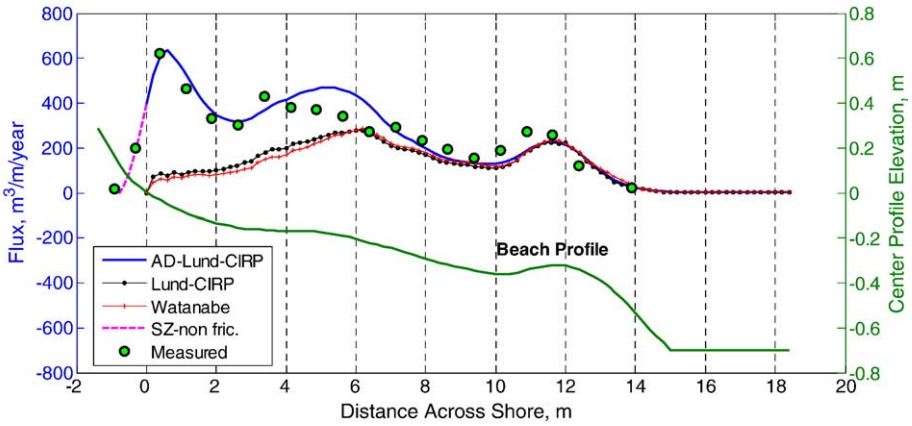

Fig. 9. Computed and measured longshore sediment flux for LSTF BC-2.

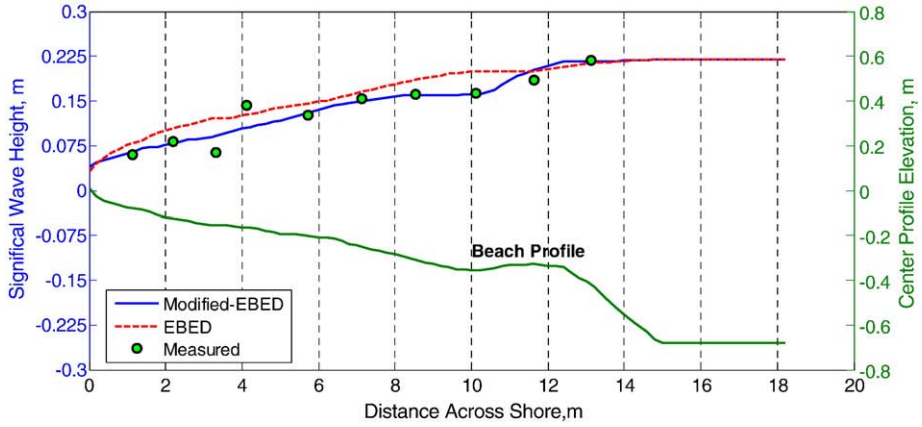

Fig. 10. Computed and measured significant wave height for LSTF BC-4.

from Eq. (5) produced good results for the Base Cases, but this equation needs to be validated with other laboratory and field data to ensure its general applicability.

Surface roller effects are necessary to include when calculating nearshore currents generated by waves. It is not only the peak of the longshore current that shifts towards the shoreline, but also the magnitude of the longshore current in the surf zone increases. The roller effects on the nearshore currents were in agreement with previously published works. By using the 2D surface roller model, energy conservation was expressed in a better manner than with the 1D model. Because the bathymetry of the LSTF basin for the Base Cases was fairly uniform, the roller energy flux alongshore in Eq. (9) was very small and could be neglected. However, this term should be included in calculations for the areas with complex bathymetry in order to obtain more accurate wave-induce currents.

Lateral mixing makes the cross-shore variation in the wave-induced longshore current smoother, and for monochromatic waves this phenomenon is needed to avoid a discontinuity at the break point. However, in the case of random waves the lateral mixing is less needed since gradual wave breaking across the profile occurs, producing a smooth forcing. Reniers and Battjes (1997) found that lateral mixing was needed to model the case of random waves breaking over a barred profile. For such a profile shape, a major portion of the waves may break on the bar and reform in the trough. In

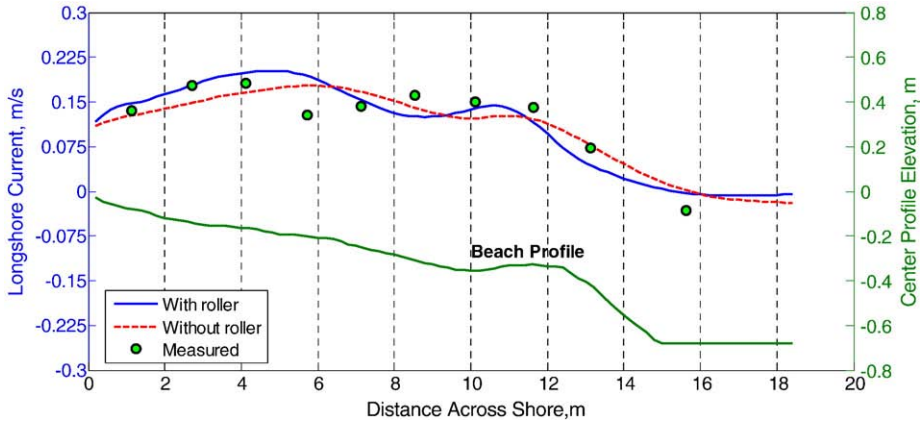

Fig. 11. Computed and measured longshore current for LSTF BC-4.

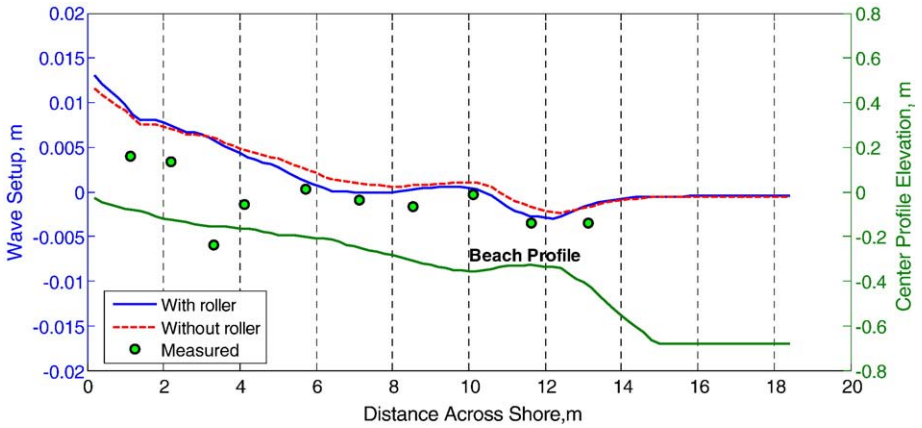

Fig. 12. Computed and measured wave setup for LSTF BC-4.

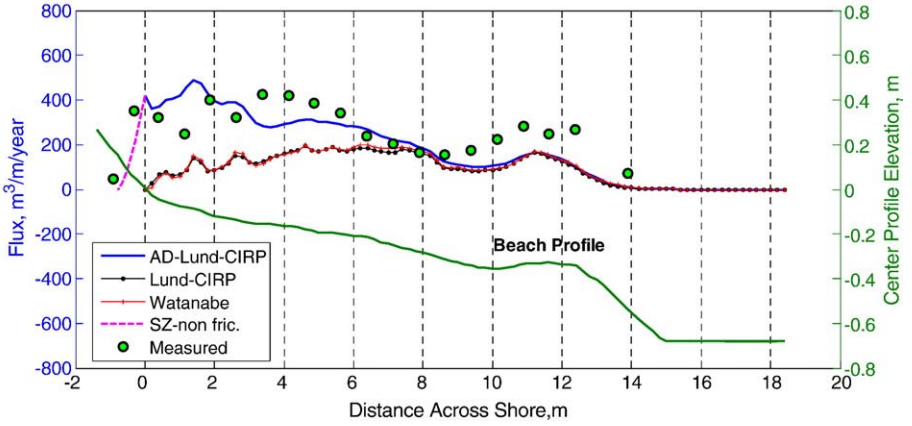

Fig. 13. Computed and measured longshore sediment flux for LSTF BC-4.

model simulations, this behavior implies little forcing in the trough and small currents here. By applying lateral mixing, this reduction in the current velocity may be counteracted. Sensitivity tests on the importance of the lateral mixing coefficient in the present study showed small effects, probably because of the profile shape changing rather gradually in the area of breaking waves.

The sediment transport typically displays great sensitivity to the roughness. Using the total roughness, including the grain-related roughness, form-drag roughness, and sediment-related roughness will produce shear stresses that may be used to calculate the sediment transport rates with some confidence. However, the formula of sediment-related roughness, which is given by Wilson (1989), is of the implicit type (for details, see Militello et al., 2006, pp. 18–20). Therefore, an iterative approach is required for solving the non-linear equation describing this roughness. In the present calculations, the Newton–Rhapson method was used for solving this equation yielding rapid convergence.

Calculating the suspended load using the advection–diffusion equation produces a smoother sediment transport rate distribution than the Lund-CIRP formula. Moreover, it can be applied to situations where suspended sediment concentration changes in time and space at a high rate, for example, at river mouths, tidal inlets, and in the vicinity of structures. Another advantage of the advection–diffusion equation is that the model uses the sediment transport rate at shoreline from the swash-zone calculations as the boundary condition for computing the suspended sediment transport in the inner surf zone.

The swash uprush and backwash occur rapidly and frequently in the swash zone, which may induce increased transport rates in the inner surf zone. If the pick-up and deposition rates were not modified ($\vartheta = 0$), the distribution of the longshore sediment transport rate would drop at a high rate seaward of the still-water shoreline, and then be similar to the calculation with the Lund-CIRP formula. Thus, it would not agree well with the investigated measured data near the shoreline. The calibration of the coefficients ϑ and μ was made for BC-1 using a range of values. The sensitivity to these coefficients is shown in Fig. 14. Based on the calibrated values for ϑ and μ, we calculated the longshore sediment flux for BC-2 and BC-4. The calibration showed that $\vartheta = 9.3$ and $\mu = 2.4$ were the most suitable values. Nevertheless, the modification of the formulas introduced and the optimal coefficient values should be validated with further data to improve the accuracy calculation of sediment transport not only for laboratory but also for field conditions.

Table 3
Root-mean-square error (%) for significant wave height, longshore current, and wave setup.

Data sets	H_s Modified-EBED	H_s EBED	v With roller	v Without roller	η With roller	η Without roller
BC-1	3.64	12.96	27.20	29.81	32.50	24.32
BC-2	3.92	14.12	17.61	19.57	51.42	52.04
BC-4	11.47	18.53	20.76	18.47	151.31	158.29

Table 4
Root-mean-square error (%) for longshore sediment transport flux.

Data sets	AD-Lund-CIRP	Lund-CIRP	Watanabe
BC-1	33.21	49.12	49.64
BC-2	18.34	59.23	62.72
BC-4	34.73	59.08	58.83

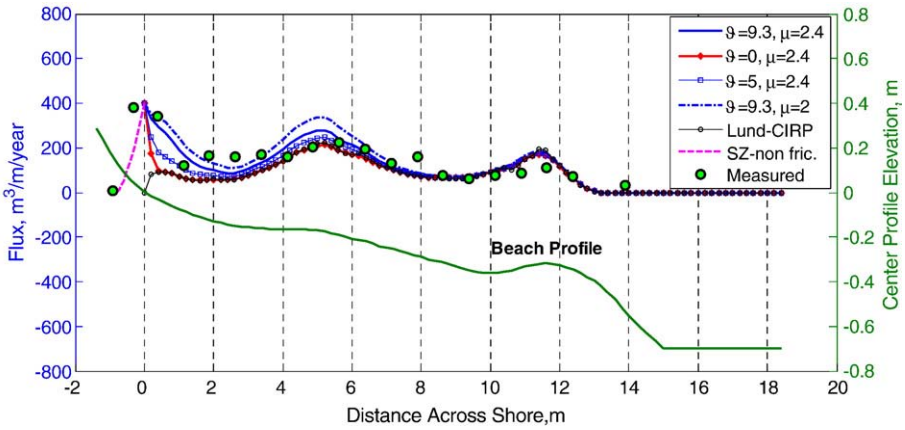

Fig. 14. Sensitive of coefficients ϑ and μ to sediment transport rate for LSTF BC-1.

7. Conclusions

A unified numerical model of nearshore waves, wave-induced currents, and sediment transport was developed. The energy dissipation due to wave breaking in the spectral wave transformation model EBED (Mase, 2001) was modified based upon the Dally et al. (1985) model, producing better predictions of the wave parameters in the surf zone. The evolution of the surface roller associated with the wave breaking after Dally and Brown (1995) was employed and enhanced, which improves the description of wave radiation stresses inside the surf zone. Including the roller shifts the nearshore current towards the shore, yielding better agreement between calculations and measurements. Newly developed formulations for the sediment transport in both swash zone and nearshore zone were applied. The modifications of pick-up and deposition rates were effective for simulating the sediment transport in the near shoreline.

The capability of model to predict the nearshore waves, wave-induced current, and sediment transport, was evaluated by comparison with three high-quality data sets from the LSTF at the Coastal and Hydraulics Laboratory. These simulations showed that the model yields reasonable predictions for the conditions studied. Thus, the model is expected to provide reliable input for calculating the morphological evolution due to waves and currents.

Acknowledgments

This work was partly funded by Sida/SAREC in the framework of the Project VS/RDE/03 “The evolution and sustainable management in the coastal areas of Vietnam” (PTN and LXH), and partly by the Inlet Modeling System Work Unit of the Coastal Inlets Research Program, U.S. Army Corps of Engineers (ML and HH). Dr. Hajime Mase at Kyoto University kindly supplied the source code for the EBED model. Dr. Ping Wang at University of South Florida and Mr. Mark Gravens at CHL provided the experimental data from their tests, which is greatly appreciated. The authors would also like to thank Dr. Nicholas C. Kraus at the U.S Army Corps of Engineers Coastal Inlet Research Program (CIRP) for the experimental data. The authors would also like to thank Dr. Nguyen Manh Hung, and the late Prof. Pham Van Ninh for their great contributions to the Project VS/RDE/03 and comments on early drafts of this paper. Finally, the authors would also like to thank the anonymous reviewers for their valuable comments.

References

Battjes, J.A., 1972. Setup due to irregular wave. Proceedings 13th International Conference on Coastal Engineering, ASCE, Vancouver, pp. 1993–2004.
Battjes, J.A., 1975. Modeling of turbulence in the surf zone. Proceedings 2nd Symposium on Modeling and Techniques, ASCE, San Francisco, pp. 1050–1061.
Bayram, A., Larson, M., Miller, H.C., Kraus, N.C., 2001. Cross-shore distribution of longshore sediment transport: comparison between predictive formulas and field measurements. Coastal Engineering 44, 79–99.
Booij, N., Holthuijsen, L.H., Ris, R.C., 1996. The ‘SWAN’ wave model for shallow water. Proceedings 25th International Conference on Coastal Engineering, ASCE, Orlando, pp. 668–676.
Booij, N., Holthuijsen, L.H, Doorn, N., Kieftenburg, A.T.M.M., 1997. Diffraction in a spectral wave model. Proc. 3rd Int. Symposium Ocean Wave Measurement and Analysis Wave '97, ASCE, New York, pp. 243–255.
Bowen, A.J., 1969. The generation of longshore currents on a plane beach. Journal of Marine Research 27 (2), 206–215.
Camenen, B., Larroude, P., 2003. Comparison of sediment transport formulae for the coastal environment. Coastal Engineering 48, 111–132.
Camenen, B., Larson, M., 2005. A general formula for non-cohesive bed load sediment transport. Estuarine, Coastal and Shelf Science 63, 249–260.
Camenen, B., Larson, M., 2007. A unified sediment transport formulation for coastal inlet application. Technical report ERDC/CHL CR-07-1, US Army Engineer Research and Development Center, Vicksburg, MS.
Camenen, B., Larson, M., 2008. A general formula for noncohesive suspended sediment transport. Journal of Coastal Research 24 (3), 615–627.
Dally, W.R., Osiecki, D.A., 1994. The role of rollers in surf zone currents. Proceedings 24th International Conference on Coastal Engineering. ASCE, Kobe, pp. 1895–1905.
Dally, W.R., Brown, C.A., 1995. A modeling investigation of the breaking wave roller with application to cross-shore currents. Journal of Geophysical Research 100 (C12), 24873–24883.
Dally, W.R., Dean, R.G., Dalrymple, R.A., 1985. Wave height variation across beaches of arbitrary profile. Journal of Geophysical Research 90 (C6), 11917–11927.
Deigaard, R., Justesen, P., Fredsoe, J., 1991. Modeling of undertow by one-equation turbulence model. Coastal Engineering 15, 431–458.
Duncan, J.H., 1981. An experimental investigation of breaking waves produced by a towed hydrofoil. Proc. R. Soc. London vol. A377, 331–348.
Elder, J.W., 1959. The dispersion of marked fluid in turbulent shear flow. Journal of Fluid Mechanics 5, 544–560.
Elfrink, B., Baldock, T., 2002. Hydraudynamics and sediment transport in the swash zone: a review and perspectives. Coastal Engineering 45, 149–167.
Falconer, R.A., 1980. Modelling of planform influence on circulation in harbors. Proceedings 17th International Conference on Coastal Engineering. ASCE, Sydney, pp. 2726–2744.
Goda, Y., 2006. Examination of the influence of several factors on longshore current computation with random waves. Coastal Engineering 53, 157–170.
Gravens, M.B., Wang, P., 2007. Data report: laboratory testing of longshore sand transport by waves and currents; morphology change behind headland structures. Technical Report, ERDC/CHL TR-07-8, Coastal and Hydraulics Laboratory, US Army Engineer Research and Development Center, Vicksburg, MS.
Gravens, M.B., Wang, P., Kraus, N.C., Hanson, H., 2006. Physical model investigation of morphology development at headland structures. Proceedings 30th International Conference on Coastal Engineering. World Scientific Press, San Diego, pp. 3617–3629.
Hamilton, D.G., Ebersole, B.A., 2001. Establishing uniform longshore currents in large-scale sediment transport facility. Coastal Engineering 42 (3), 199–218.
Holthuijsen, L.H., Herman, A., Booij, N., 2003. Phase-decoupled refraction–diffraction for spectral wave models. Coastal Engineering 49, 291–305.
Hunt, I.A., 1959. Design of seawalls and breakwaters. Journal of Waterways and Harbors Division 85, 123–152.
Kraus, N.C., Larson, M., 1991. NMLONG: Numerical model for simulating the longshore current; report 1: model development and tests. Technical Report DRP-91-1, U.S. Army Engineer Waterways Experiment Station, Vicksburg, MS.
Larson, M., Kraus, N.C., 2002. NMLONG: numerical model for simulating longshore current; report 2: wave–current interaction, roller modeling, and validation of model enhancements. Technical Report ERDC/CHL TR-02-22, US Army Engineer Research and Development Center, Vicksburg, MS.
Larson, M., Wamsley, T.V., 2007. A formula for longshore sediment transport in the swash. Proceedings Coastal Sediments '07. InASCE, New Orleans, pp. 1924–1937.

Larson, M., Kubota, S., Erikson, L., 2004. Swash-zone sediment transport and foreshore evolution: field experiments and mathematical modeling. Marine Geology 212, 61–79.
Lippmann, T.C., Brookins, A.H., Thornton, E.B., 1996. Wave energy transformation on natural profiles. Coastal Engineering 27, 1–20.
Longuet-Higgins, M.S., 1970. Longshore current generated by obliquely incident sea waves. Journal of Geophysical Research 75 (33), 6779–6801.
Longuet-Higgins, M.S., Stewart, R.W., 1964. Radiation stresses in water waves; a physical discussion with applications. Deep Sea Research 11, 529–562.
Madsen, P.A., Warren, I.R., 1984. Performance of a numerical short-wave model. Coastal Engineering 8, 73–93.
Madsen, P.A., Murray, R., Sorensen, O.R., 1991. A new form of the Boussinesq equations with improved linear dispersion characteristics. Coastal Engineering 15, 371–388.
Madsen, P.A., Sorensen, O.R., Schäffer, H.A., 1997. Surf zone dynamics simulated by a Boussinesq type model. Part II: surf beat and swash oscillations for wave groups and irregular waves. Coastal Engineering 32, 289–319.
Mase, H., 2001. Multi-directional random wave transformation model based on energy balance equation. Coastal Engineering Journal 43 (4), 317–337.
Militello, A., Reed, C.W., Zundel, A.K., Kraus, N.C., 2004. Two-dimensional depth-averaged circulation model M2D: version 2.0, report 1, technical document and user's guide. Technical Report ERDC/CHL TR-04-2, Coastal and Hydraulics Laboratory, US Army Engineer Research and Development Center, Vicksburg, MS.
Militello, A., Reed, C.W., Kraus, N.C., Ono, N., Larson, M., Camenen, B., Hanson, H., Wamsley, T., Zundel, A.K., 2006. Two-dimensional depth-averaged circulation model CMS-M2D: version 3.0, report 2,sediment transport and morphology change. Technical Report ERDC/CHL TR-06-9, Coastal and Hydraulics Laboratory, US Army Engineer Research and Development Center, Vicksburg, MS.
Nairn, R.B., Roelvink, J.A., Southgate, H.N., 1990. Transition zone width and implications for modeling surfzone hydrodynamics. Proceedings 22nd International Conference on Coastal Engineering. ASCE, Delft, pp. 68–81.
Nishimura, H., 1988. Computation of nearshore current. In: Horikawa, K. (Ed.), Nearshore Dynamics and Coastal Processes. InUniversity of Tokyo Press, Tokyo, Japan, pp. 271–291.
Nwogu, O., 1993. Alternative form of Boussinesq equations for nearshore wave propagation. Journal of Waterway, Port, Coastal, and Ocean Engineering 119 (6), 618–638.
Reniers, A.J.H.M., Battjes, J.A., 1997. A laboratory study of longshore currents over barred and non-barred beach. Coastal Engineering 30, 1–22.
Rivero, F.J., Arcilla, A.S, Carci, E., 1997. Analysis of diffraction in spectral wave models. Proc. 3rd Int. Symposium Ocean Wave Measurement and Analysis Wave '97. ASCE, New York, pp. 431–445.
Ruessink, B.G., Miles, J.R., Feddersen, F., Guza, R.T., Elgar, S., 2001. Modeling the alongshore current on barred beaches. Journal of Geophysical Research 106 (C10), 22451–22463.
Soulsby, R.L., 1997. Dynamics of marine sands. Thomas Telford, HR Wallingford, London.
Stive, M.J.F., De Vriend, H.J., 1994. Shear stresses and mean flow in shoaling and breaking waves. Proceedings 24th International Conference on Coastal Engineering. ASCE, Kobe, pp. 594–608.
Svendsen, I.A., 1984a. Wave heights and set-up in a surf zone. Coastal Engineering 8, 303–329.
Svendsen, I.A., 1984b. Mass flux and undertow in a surf zone. Coastal Engineering 8, 347–365.
Takayama, T., Ikeda, N., Hiraishi, T., 1991. Wave transformation calculation considering wave breaking and reflection. Rept. Port Harbor Res. Inst. 30 (1), 21–67.
Thornton, E.B., 1970. Variation of longshore current across the surf zone. Proceedings 12th International Conference on Coastal Engineering. ASCE, Washington D.C., pp. 291–308.
Thornton, E.B., Guza, R.T., 1983. Transformation of wave height distribution. Journal of Geophysical Research 88 (C10), 5925–5938.
Thornton, E.B., Guza, R.T., 1986. Surf zone longshore currents and random waves: field data and models. Journal of Physical Oceanography 16, 1165–1178.
Van Dongeren, A., Sancho, F.E., Svendsen, I.A., Putrevu, U., 1994. SHORECIRC: a quasi 3-D nearshore model. Proceedings 24th International Conference on Coastal Engineering. ASCE, Kobe, pp. 2741–2754.
Van Dongeren, A., Svendsen, I.A., 2000. Nonlinear and 3D effects in leaky infragravity waves. Coastal Engineering 41, 467–496.
Van Dongeren, A., Reniers, A., Battjes, J., 2003. Numerical modeling of infragravity wave response during DELIAH. Journal of Geophysical Research 108 (C9), 3288. doi:10.1029/2002JC001332.
WAMDI group, 1988. The WAM model-a third generation ocean wave prediction model. Journal of Physical Oceanography 18, 1775–1810.
Wang, P., Ebersole, B.A., Smith, E.R., Johnson, B.D., 2002. Temporal and spatial variations of surf-zone currents and suspended sediment concentration. Coastal Engineering 46, 175–211.
Watanabe, A., 1987. 3-dimensional numerical model of beach evolution. Proceedings Coastal Sediments '87. ASCE, pp. 802–817.
Wilson, K.C., 1989. Friction of wave-induced sheet flow. Coastal Engineering 12, 371–379.